Experimental Mechanical Property Investigation on PLA-CF Specimens using Fused Filament Fabrication Technology

Hind B. Ali
College of Material Engineering, University of Technology-Iraq, Iraq
130047@uotechnology.edu.iq (corresponding author)

Dalia J. Al Ibadi
Dijlah University College, Iraq
daly_jb@yahoo.com

Hawraa Dheaaldin
College of Material Engineering, University of Technology-Iraq, Iraq
130219@uotechnology.edu.iq

Shams B. Ali
College of Laser and Optoelectronics Engineering, University of Technology-Iraq, Iraq
shams.b.ali@uotechnology.edu.iq

Muhammad Qasim Sharhan
College of Material Engineering, University of Technology-Iraq, Iraq
jadded50@gmail.com

Farah Moataz Abdel Salam
College of Material Engineering, University of Technology-Iraq, Iraq
engf888@gmail.com

Zainab Salam Hashem
College of Material Engineering, University of Technology-Iraq, Iraq
mae.19.074@student.uotechnology.edu.iq

Received: 6 January 2025 | Revised: 28 February 2025, 19 March 2025, and 12 April 2025 | Accepted: 22 April 2025

 DOI: https://doi.org/10.48084/etasr.10111

ABSTRACT

This study investigated the mechanical characteristics of components produced from composite Polylactic Acid reinforced with Carbon Fibers (PLA-CF). PLA and PLA-CF were produced with strict rules regarding layer thickness, nozzle diameter, printing speed, and orientation. PLA-CF exhibited superior tensile characteristics, Izod impact test values, and higher crystalline degree than PLA. Samples with density values of 20%, 40%, 60%, 80%, and 100% were tested for ultimate tensile strength. It was shown that the PLA-CF UTS samples at 100% infill density (45.292 MPa) surpassed the PLA samples (42.235 MPa). As the strength values increased, the Izod impact strength followed the same pattern with infill density. The Grey Relational Analysis (GRA) approach was employed to optimize the infill density in order to enhance the dimensional accuracy. The aforementioned parameter was found to have a more significant influence on product quality and time reduction in the Fused Filament Fabrication (FFF) process.

Keywords-Fused Filament Fabrication (FFF); PLA-CF; tensile strength; Izod strength test; grey relational analysis

I. INTRODUCTION

The constraints placed on the development and production processes are becoming increasingly demanding in the modern setting markets. Besides the criteria that are being established to improve product quality and flexibility in development and production, additional requirements are being imposed to minimize costs, with a particular focus on decreasing the time amount spent on development and production. In some market niches, a new trend, which is becoming increasingly significant, is the mass abandoning manufacturing in a smaller production favor scale and usually on an individual basis (also known as personalized production) [1]. Fused Filament Fabrication (FFF) has been deployed to manufacture any item, ranging from a simple to a highly complicated form, using a simple software program and polymeric materials, which possess the desirable mechanical and thermal qualities. This technology has attracted the attention of academic researchers and businesspeople due to its capacity to produce sophisticated structures in a short time [2, 3]. Three dimensional (3D)-printing is a relatively new technology, which includes the material addition in successive layers in order to produce items with a high-quality finish [4].

In the additive manufacturing process, the machine is given instructions to deposit material in exact geometric patterns, often known as consecutive layers. This is accomplished via Computer-Aided Design (CAD) software or 3D object scanners. Some thermoplastic polymers and reinforced materials that can be printed employing Fused Deposition Modeling (FDM) are ABS, PLA, polycarbonate, Ultem, PEEK, and fiber-reinforced thermoplastics [5, 6]. Components manufactured using FDM are gradually replacing traditional components in a number of different industries. PLA's applicability in various sectors is, however, severely limited due to the fact that it is brittle and resistant to low temperatures [7]. Therefore, the enhancement of PLA's mechanical performance has been a goal pursued in both the academic and industrial sectors. It has been specifically determined that the primary cause of the inadequate mechanical properties of PLA is its limited crystallization ability [8]. As a consequence, attempts have been made to improve PLA with fibers in order to enhance its crystallization. In [9], it was proven that fibers have the ability to successfully promote crystallization and greatly increase matrix properties. As indicated in [6, 8], the process variables and their parameters have a considerable influence on the mechanical properties of manufactured FDM printed components [10-13]. In general, the fibers used to strengthen PLA may be obtained from either natural or synthetic sources [14]. Therefore, in order to enhance the mechanical characteristics for printed components, it is essential to analyze the influence of the elements entered into the process and predict the outcomes by utilizing the right process parameters [15]. Authors in [16] investigated the influence of different printing settings on material tensile strength employing PLA filament. Based on the obtained data, in addition to the construction orientation and raster orientation, these parameters included nozzle diameter, infill density, and build orientation. It was found that all of them had a substantial effect on the component's strength, with the latter having the most essential influence. Infill density, layer height, print speed, and fill pattern significantly affect the FDM component's tensile strength [17]. In [18], an evaluation was conducted for the thermoplastic mechanical characteristic's materials and reinforced polymers. Several context infill patterns were used, such as concentric, zig-zag, and four separate orientations. In FFF, basic and support materials may be extruded utilizing the same nozzle or another one, depending on the 3D printer equipment [19]. This is possible because the nozzle can be employed in various ways. When some conditions are met, the fiber is deposited on the specimen top, which has been partly manufactured [20]. When evaluating the mechanical response on the specimen obtained through this process, it is necessary to take into consideration various parameters, including layer height, nozzle diameter, raster angle [15, 21], or infill pattern [21, 22] to the melted filaments [23], for both the pure polymer and fiber in a composite material, along with infill density [11, 24-27].

Among the additive manufacturing techniques based on the melt extrusion approach, FFF utilization is becoming more common [25, 27, 28], as shown in Figure 1. These methods include the extrusion for the molten material, which is often in the form on the filaments, through openings with the various diameters in order to generate certain components, significantly contributing to growth potential [25, 29].

This research aims to determine an acceptable filling density for the discussed parameters and analyze the mechanical quality influence on the specimens generated by the FDM technology. During the FDM specimen manufacturing process, the designer has control over the print speed, layer thickness, shell thickness, and printing orientation. Utilizing the Taguchi optimization technique, the present work also intends to evaluate the influence that the process parameters have on the mechanical characteristics of the samples. Scanning Electron Microscopy (SEM) was used to examine the fracture surface of the selected specimens, and thus identify the failure cause.

II. METHODOLOGY

A. Materials and Process Parameters

FDM works best with polymers that are amorphous in nature [30] rather than with highly crystalline polymers, which are more suitable for the processes illustrated in Figure 2.

1) Polylactic Acid

PLA is a biodegradable material derived from natural resources, such as maize starch. Its popularity for prototype and hobbyist 3D printing stems from its user-friendly nature and eco-friendly characteristics.

2) Carbon Fiber Reinforced Polymers (CFRPs)

Due to their high strength-to-weight ratio, CFRP composites are used to manufacture components that are both lightweight and sturdy. The specimen for the tensile test was built as a CAD geometric model, as depicted in Figure 3.

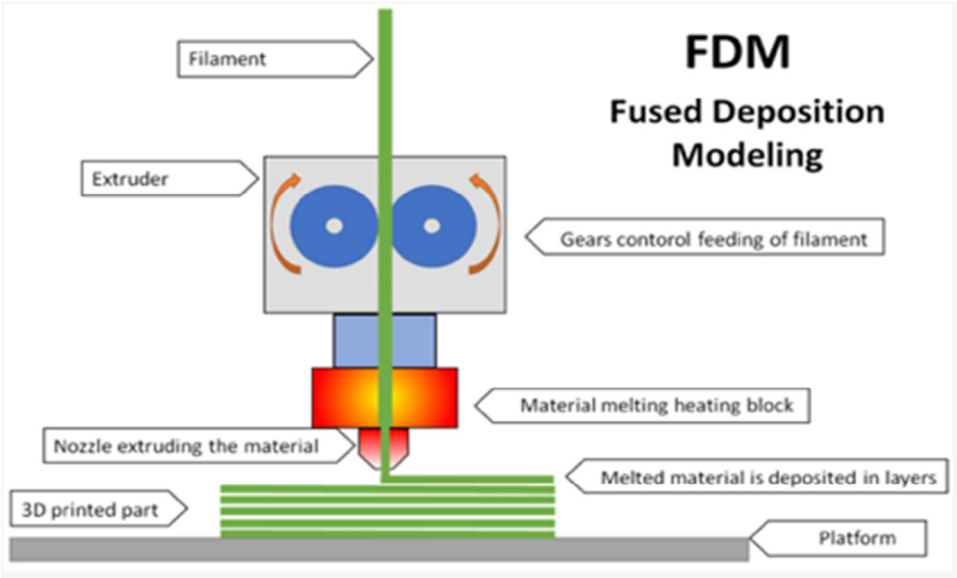

Fig. 1. 3D printing diagram process using the FDM technique.

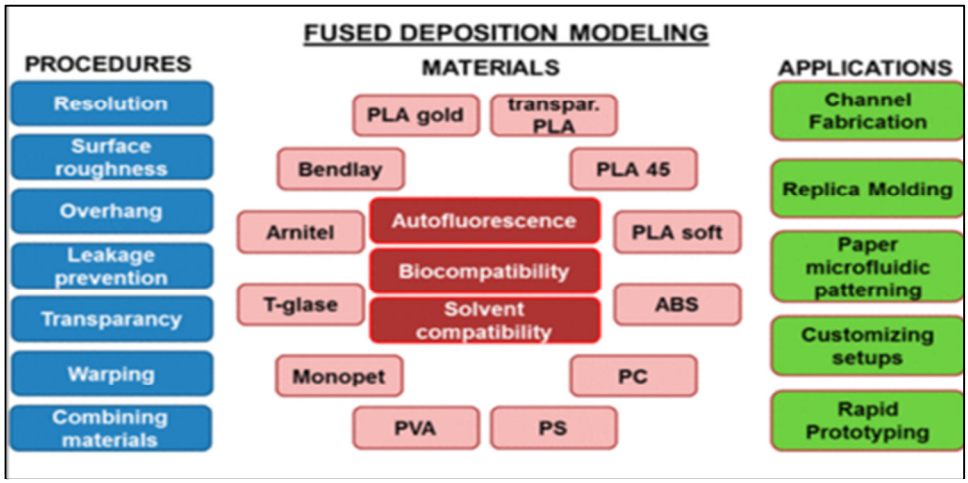

Fig. 2. FDM materials.

Fig. 3. Specimens for (a) tensile test, (b) Izod impact test.

All specimens were made according to the requirements of the ASTM D638-02a standard (Type I specimen, 7 mm length). The Izod test is a standard procedure to assess the influence of a material's resistance according to ISO180. The Un-notched Izod impact test allows for the measurement of material resistance on the swing pendulum. This test is performed at a single site. The kinetic energy required to initiate fracture and failure is measured and reported. For this research, 3D printing machines equipped with FFF technology were used. To produce pure polymer and composite component specimens, the Ultimaker 2+ printer (Ultimaker, Utrecht, Netherlands) was used, as portrayed in Figure 4. In order to create the specimens, a filament consisting of PLA and PLA-CF with a diameter of 2.85 ± 0.05 mm, manufactured in China, was used.

B. Mechanical Test

Both tensile and Izod test specimens comprised two sets of PLA and PLA-CF combinations, as shown in Figure 5.

The considered parameters were: Layer thickness of 0.1 mm height, nozzle diameter of 0.6 mm, print speed of 40 mm/sec, orientation of 45^{o}, and infill densities of 20%, 40%, 60%, 80%, and 100%. One of the most distinguishing characteristics of the CF test specimens is the smooth surface texture they possess. Tests were carried out for each parameter until at least three sets among the consistent data were acquired and the average values were reported as the results. The specimens were grouped according to the density of the filling, as outlined in Table I.

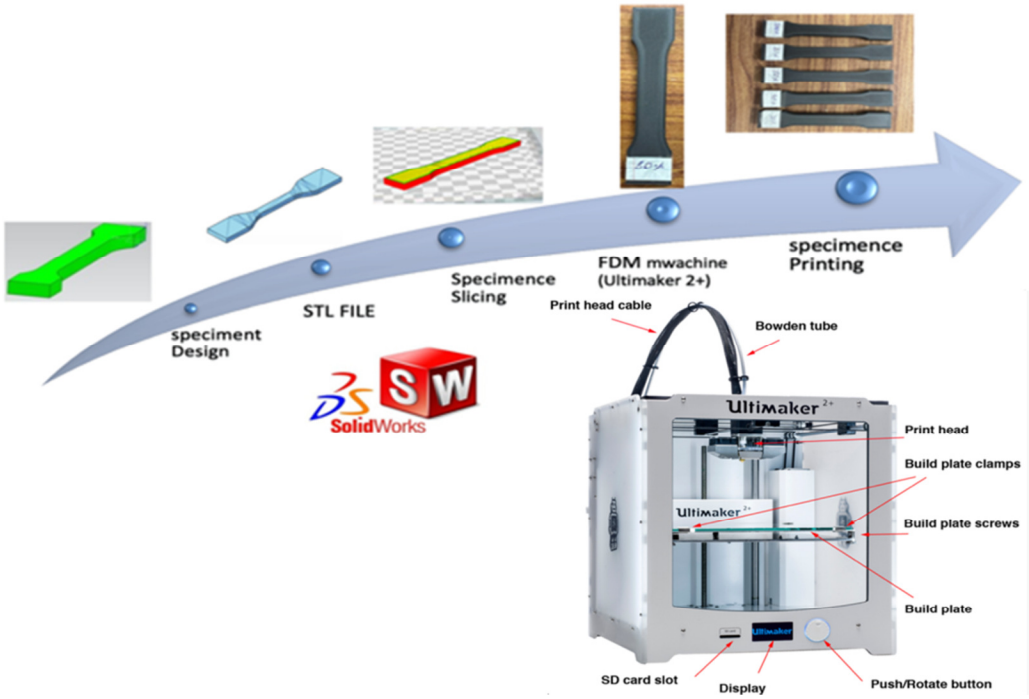

Fig. 4. Part manufacturing steps.

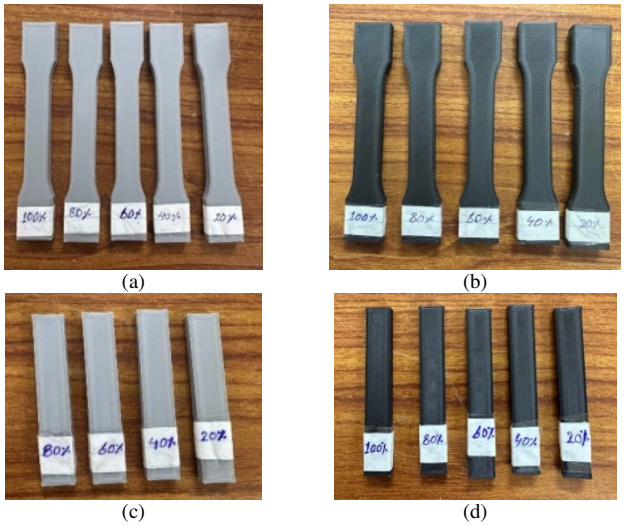

Fig. 5. Test samples: (a) PLA tensile specimen, (b) PLA-CF tensile specimen, (c) PLA impact specimen, (d) PLA-CF impact specimen.

TABLE I. FACTORS AND THEIR LEVELS

Fixed factors			**Control factors**		
Factor	Value	Unit	Factor	Value	Unit
Layer thickness	0.1	Mm	Infill density	20	%
Nozzle diameter	0.6	Mm		40	
Print speed	40	Mm/s		60	
Part orientation	45	Degree		80	
				100	

1) Tensile Test

The specimens were subjected to tensile test in accordance with [31]. The tests were carried out using a tensile strength machine, as shown in Figure 6. The cross-head speed (strain rate) was set at 5 mm/min, and the load was set at 5 kN.

2) Impact Test

The Izod test is a part of the ISO180 standard for determining the resistance of a material. Un-notched Izod impact is a one-point test that examines the material's resistance to the impact from a swing pendulum, as depicted in Figure 7.

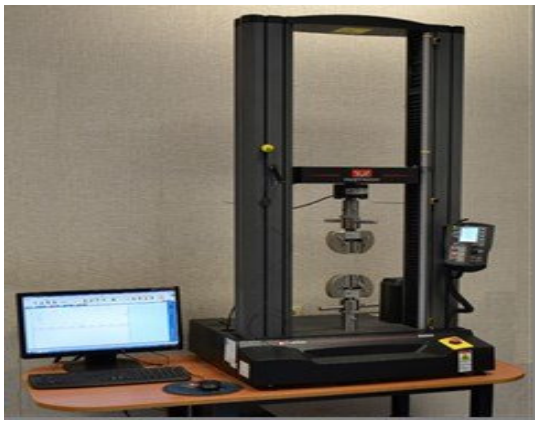

Fig. 6. Universal tensile testing machine.

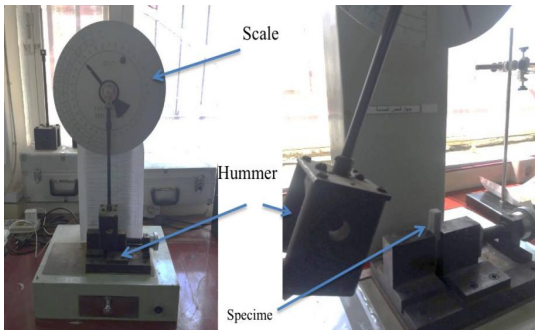

Fig. 7. Impact test machine.

The impact strength (J) is calculated [22] by:

$$\text{Impact Strength} = \frac{\text{Impact Energy}}{\text{Cross-Sectional Area}} \quad (1)$$

where the Impact Energy and Cross-Sectional Area are measured in J and m^2, respectively.

C. Physical Properties

1) Dimensional Accuracy Test

To determine the length (l), width (w), and thickness of the object, a digital caliper with a least count of 0.01 mm was used to accurately measure the dimensions. The relative change in dimensions was calculated by [18]:

$$\Delta x = \frac{x - x_{CAD}}{x_{CAD}} \quad (2)$$

where x is the measured value of length, width, or thickness, x_{CAD} is the designed or ideal value from the CAD model, and Δx indicates the relative change in x.

2) Grey Relational Analysis

After data pre-processing, the grey relational coefficient is derived from (3) [19], and then the original sequence is normalized [32]:

$$x_i^*(k) = \frac{max\, x_i(k) - x_i(k)}{\max x_i(k) - \min x_i(k)} \quad (3)$$

where $x_i^*(k)$ and $x_i(k)$ are the sequences following the data comparability sequence and preprocessing, respectively. Also, k=1 for each mechanical characteristic, i takes the values of 1, 2, 3, 4, and 5, representing the experiments from 1 to 5.

The deviation sequence $\Delta_i(k)$ is defined by [33]:

$$\Delta_i(k) = \left| x_0^*(k) - x_i^*(k) \right| \quad (4)$$

where $x_0^*(k)$ and $x_i^*(k)$ are the reference sequence and the comparability sequence, respectively.

The pre-processed sequence describes the relationship between the actual normalized experimental data and the ideal. The grey relational coefficient $\varepsilon_i(k)$ is calculated by [34]:

$$\varepsilon_i(k) = \frac{\Delta_{min} + \varepsilon\Delta_{max}}{\Delta_i(k) + \varepsilon\Delta_{max}} \quad (5)$$

where $\Delta_i(k)$ represents the series on deviations from the reference sequence and ε is the coefficient used to identify or differentiate between two variables [35].

The grey relational grade γ_i is calculated by taking the average of the grey relational coefficients that correspond to each performance characteristic. This occurs after the grey relational coefficient has been determined. In order to arrive at the grey relational grade, an analysis on a large number of performance characteristics is performed using [36]:

$$\gamma_i = \frac{1}{p}\sum_{k=1}^{n} \mathrm{E}_i(k) \quad (6)$$

where i is the number of the experiments and p is the number of performance characteristics.

III. RESULTS AND DISCUSSION

A. Results of Mechanical Properties

1) Tensile Strength

The tensile test results can be seen in Table II. The UTS graph relevant to the filling density of PLA and PLA-CF filaments is presented in Figure 8.

TABLE II. UTS RESULTS.

Filling density	UTS PLA-CF	UTS PLA
20%	18.554	12.721
40%	26.61	21.736
60%	30.732	23.543
80%	33.124	32.012
100%	45.292	42.235

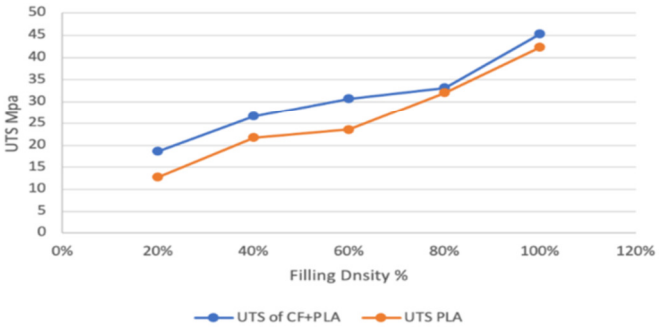

Fig. 8. UTS in relation to the filling density.

The filling density is a significant process parameter with a substantial influence on the mechanical characteristics of the material. In accordance with the criteria established by the ASTM, the ultimate strength values were determined by calculating the average measurement results. After that, the stress, and PLA and PLA-CF strain values were evaluated across five different filling density levels to identify which material was the most robust. Then, the stress-strain diagrams for five distinct PLA infill patterns and five different PLA-CF infill patterns were extracted, as shown in Figures 9 and 10.

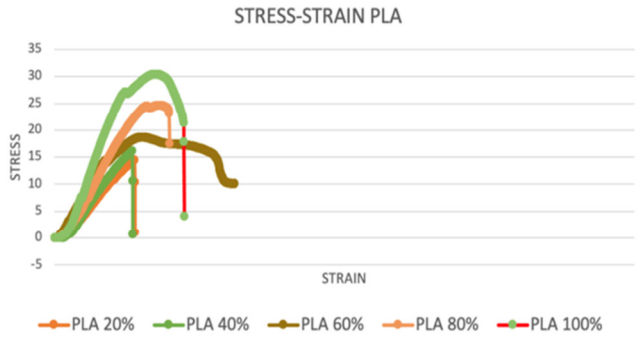

Fig. 9. The stress-strain curve for PLA specimens.

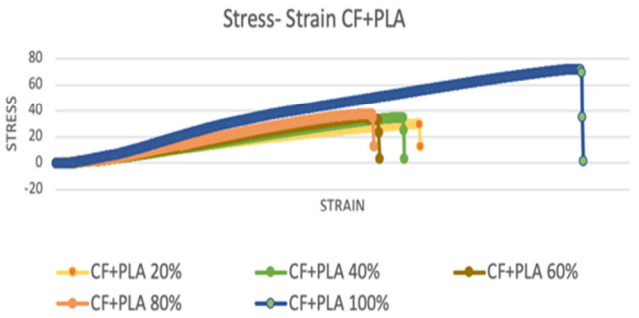

Fig. 10. The stress-strain curve for PLA-CF tensile specimens.

The test results demonstrated that a 100% infill density produced the maximum tensile strength, with values of 45.292 MPa for PLA-CF and 42.235 MPa for PLA.

By locating the greatest value on the stress-strain diagram, it will be possible to get the final stress value in a quick and effective manner. The filling density with the lowest tensile strength among the five specimens is 38.554 MPa for PLA-CF, whereas the filling density with the highest tensile strength is 22.721 MPa for the PLA filament. Due to the fact that it is composed of 20% printed components, it has a low tensile strength and is prone to breaking when put in strain. Therefore, while developing a 3D printed component or specimen of PLA-CF material deploying FDM technology, which is capable of handling high tensile strength, it is advised to use 100% material for better outcomes under the described operating conditions. PLA-CF has a higher tensile strength of 45.292 MPa than PLA, which has 42.235 MPa, when the infill density is the same.

2) Impact Strength

The purpose of this study was to measure the impact strength on composites made of PLA and PLA-CF. To analyze and assess the numerical data, the performance characteristic used for this investigation is the impact strength that was established by the Izod impact test on the FDM-produced PLA and PLA-CF samples. High Izod influence strength demonstrates that the specimens are able to maintain their stability even after being subjected to impact. The results are displayed in Table III.

According to the test results, the average impact strength values for the PLA materials range from 30.709 kJ/m^2 to 77.098 kJ/m^2, while the values for PLA-CF range from 43.924 kJ/m^2 to 90.963 kJ/m^2. When compared to the findings of the research on the Izod impact strength on PLA and PLA-CF generated by FDM, the overall impact strength results for PLA-CF are comparatively high, as illustrated in Figure 11. It is a common knowledge that the greater the percentage of infill density is, the better is the strength (along with the material consumption, weight, and print time), but the lesser is the experienced flexibility.

TABLE III. IMPACT STRENGTH RESULTS

Filling Density	Influence strength kJ/m^2 PLA	Influence strength kJ/m^2 PLA-CF
20%	30.709	43.924
40%	45.332	64.836
60%	50.376	76.024
80%	65.907	84.923
100%	77.098	90.963

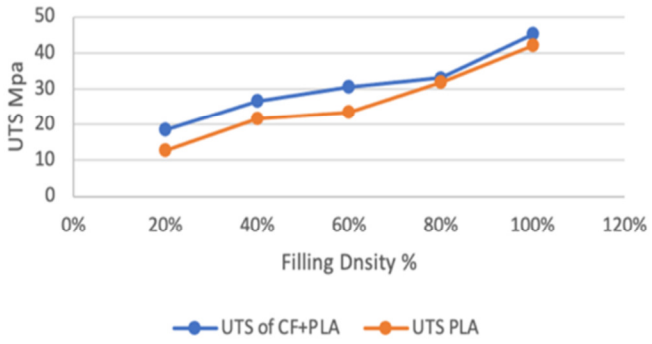

Fig. 11. Izod Impact strength in relation to the infill density.

Perfect infill density of 100% is the printing parameter value that yields the maximum Izod strength. It is clear that high infill density levels increase the PLA-CF Izod impact strength, making it superior to PLA's. The material impact strength is significantly affected by an increase in the material density, as well as a reduction in the void amount and porosity, as compared to other levels of 100% infill density. Authors in [29] found that the impact strength increased up to 100% with filler concentrations.

B. Physical Properties

1) Dimensional Accuracy

The divergence from the fundamental dimensions of the specimen is what is meant by the term "dimensional accuracy." All mechanical property tests examine the specimen in length, width, and thickness. According to the measured data, on practically every occasion, the expected value by the CAD model is exceeded by the shrinkage that occurs in the length, width, and thickness. The change in dimension is computed by (2), and the outcomes are shown in Table IV.

The experimental findings about the change in dimension value are calculated by (3), and are presented in Table V, which illustrates that the model is adequate since there is only a little variation between the expected and the observed values for ΔL, ΔW, and ΔT. Since all performance characteristics that

were investigated are lower for the better type, the grey relational generation is approximated using (4). The grey relation coefficient results are shown in Table VI, with a distinguishing coefficient of 0.5.

TABLE IV. RELATIVE CHANGE IN DIMENSION FOR MECHANICAL PROPERTIES.

Sample no.	Impact strength			Tensile strength		
	ΔL	ΔW	ΔT	ΔL	ΔW	ΔT
1	0.000667	0.001	0.005	0.00513	0.085	0.095
2	0.000500	0.002	0.003	0.00380	0.065	0.009
3	0.000500	0.005	0.002	0.00227	0.088	0.097
4	0.000833	0.003	0.004	0.00660	0.041	0.001
5	0.000667	0.004	0.007	0.00287	0.003	0.092

TABLE V. DIMENSION PERFORMANCE CHARACTERISTICS

Sample no.	Impact strength			Tensile strength		
	ΔL	ΔW	ΔT	ΔL	ΔW	ΔT
1	0.223	0.000	0.661	0.945	0.990	0.991
2	0.176	0.431	0.292	0.880	0.930	0.478
3	0.176	1.000	0.000	0.767	0.997	0.996
4	0.258	0.683	0.500	1.000	0.827	0.000
5	0.223	0.861	0.904	0.819	0.245	0.984

TABLE VI. GRAY RELATIONAL COEFFICIENT

Sample no.	Impact strength			Tensile strength		
	ΔL	ΔW	ΔT	ΔL	ΔW	ΔT
1	0.391	0.333	0.596	0.901	0.980	0.982
2	0.378	0.468	0.414	0.806	0.877	0.489
3	0.378	1.000	0.333	0.683	0.995	0.991
4	0.403	0.612	0.500	1.000	0.743	0.333
5	0.391	0.783	0.838	0.734	0.398	0.969

Each performance criterion is given the same amount of weight in the calculation at the grey relation grade, which is calculated by (6). The results are illustrated in Table VII.

TABLE VII. DIMENSION GREY RELATIONAL GRADE

Sample no.	Length	Width	Thickness	Grade
1	0.611	0.63	0.535	3
2	0.522	0.708	0.405	2
3	0.632	0.839	0.715	1
4	0.471	0.622	0.436	5
5	0.63	0.626	0.683	4

The findings indicate that the width has a greater influence than the other dimensions, with sample 3 having the greatest influence with a filling density of 60%, followed by sample 5 with 40% and 1 with 20%, while samples 4 and 5 with 80% and 100%, respectively, did not have a significant influence, as shown in Figure 12.

The analysis determined the filling density percentage length (Figure 13(a)). The influence of the filling density at 60% and 100% is the same, while a density of 20% seems to have a comparable effect on the samples' mechanical properties. On the other hand, samples with 40% and 80% density have low influence (Figure 13(b)).

Filling density of 60% has a significant influence on the samples' mechanical properties, while 40% seems to have a comparable influence. Other samples with filling densities of 20%, 80%, and 100% have an influence that is either minor or nonexistent. According to the study findings, the fracture is determined by thickness, as depicted in Figure13(c).

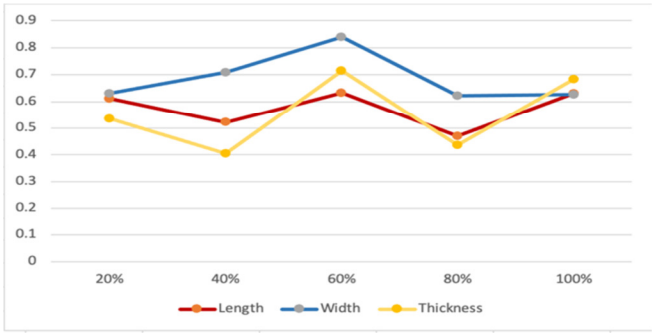

Fig. 12. Dimensional accuracy using GRA for mechanical properties.

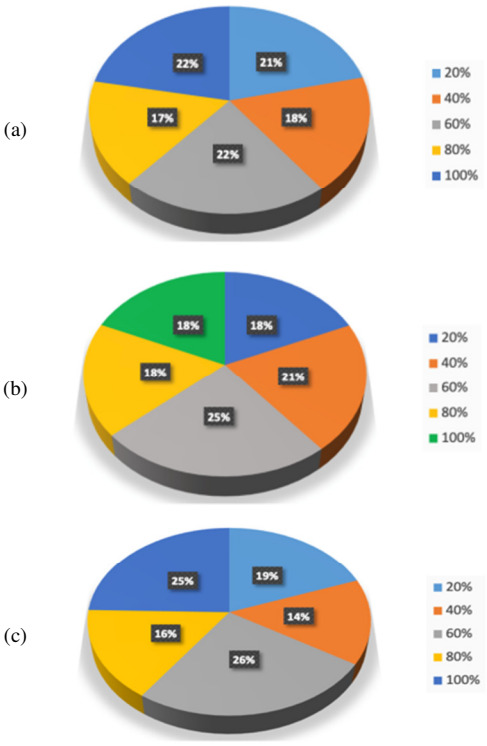

Fig. 13. Infill Density's percentage contributions to dimensional accuracy: (a) length, (b) width, (c) thickness.

2) Scanning Electron Microscope Test

a) Tensile Strength

An examination of the morphology of samples was carried out with the assistance of SEM. Gold coating was applied to the surface of the sample in order to avoid surface charging, as can be seen in Figure 14. The PLA and PLA-CF samples, both having an infill density of 100%, had a fracture surface that was pitted and rough. There was a more ductile fracture, which occurred suddenly in the smooth zone in the PLA-CF specimen, as shown in Figures 14(c-d).

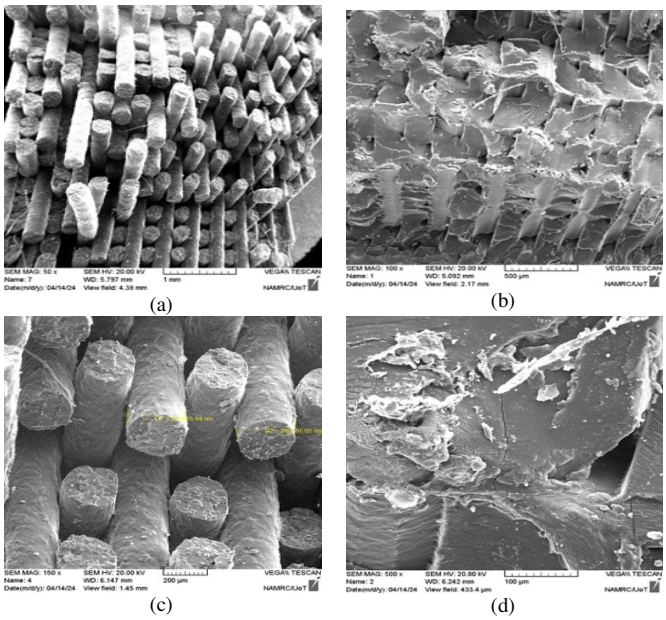

Fig. 14. SEM test at 100% filling density:(a, b) fracture surfaces of the PLA specimen, (c, d) fracture surfaces of the PLA-CF specimen.

b) Impact Strength

SEM was deployed to investigate the cracked surfaces of the PLA and PLA-CF. The micrographs observed in Figure 15 demonstrate that the carbon fibers were partially adhered to the PLA. In spite of the fact that the investigated FDM samples had apparent CF clumps, the SEM scans revealed individual fibers that were well-dispersed inside the PLA, as illustrated in Figure 15(d).

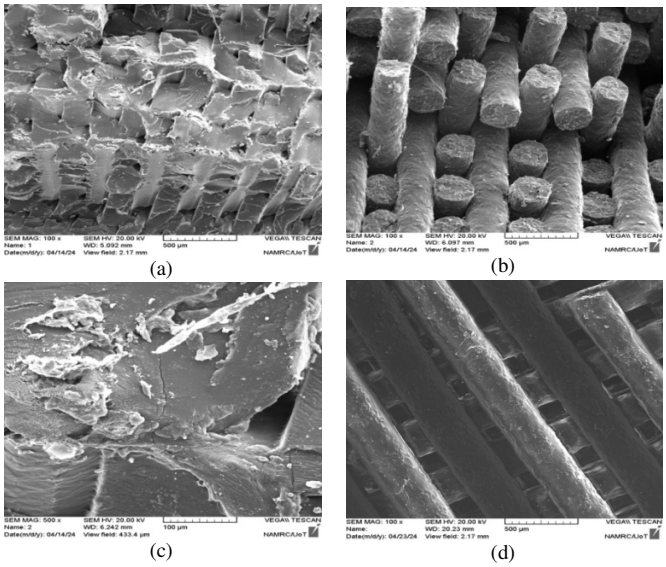

Fig. 15. Fractured surfaces of the specimens with the same magnification: (a, b) PLA, (c, d) PLA-CF.

It was discovered that there were some vacant spots between the PLA fiber and the PLA substrate. The SEM analysis showed that the FDM specimens had a high amount of fiber-matrix adhesion. The impact strength on the PLA-CF samples was found to be higher than that on the PLA samples, which may suggest that the fiber-matrix interaction is stronger or that the fiber itself is better.

IV. CONCLUSION

This study's objective was to conduct an empirical investigation on the effect of infill density on the FDM process parameters, while ensuring that all other parameters remained the same. A key parameter was discovered to be the tensile strength at the components manufactured from PLA and PLA-CF. It is important to note that the tensile strength of the FDM printed PLA-CF products is influenced by the infill density. When the infill density was 100%, the tensile characteristics were determined to be at their maximum. The following conclusions were drawn:

- The tensile strength of the PLA-CF was 45.292 MPa when the infill density was 100%, whereas the tensile strength of PLA was also 45.292 MPa.
- PLA-CF infill density was more compact because it was printed from the outside to the center of the model. This caused infill lines to be close, enhancing the uniformity of the printed layers.
- At an infill density of 20%, the tensile strength of the PLA-CF samples dropped to 18.554 MPa, while the tensile strength of the PLA samples dropped to 12.721 MPa. This is because the interlayers are weak and quickly break under tensile strain.
- The infill density percentage had a considerable influence on the outcome. Filler density was shown to have an effect on a wide range of mechanical characteristics, including ultimate tensile stress and impact strength. As a result, the stress-strain graphs also witnessed a shift.
- During the process, the fibers that have been deposited were bonded by the melting and diffusion on the previous deposited material. As a result, the component may undergo deformation and develop dimensional errors.
- Width increment may be attributed to the removal of flaws and uneven layer surfaces that were produced during the deposition process.
- Continuous carbon fiber reinforcement in combination with different infill densities to improve mechanical performance has not been extensively studied in previous studies, which commonly focus on short or chopped fiber composites. Material optimization (PLA-CF) and structural parameter change (infill density) are combined in this work to take a more thorough approach, while most previous studies considered single-variable effects or used discontinuous fibers. According to the results, continuous fiber loading greatly improves strength and impact performance, which makes it more appropriate for functional applications.
- By indicating that well defined process parameters, particularly infill density at ideal extrusion temperatures, may greatly enhance the mechanical integrity of printed composites, this study adds to the expanding corpus of

knowledge on additive manufacturing. These results provide useful direction for companies looking to move FFF-produced parts from prototypes to components that are ready for use, especially in structural, automotive, and aerospace applications.

CONFLICTS OF INTEREST

The authors declare that they have no known competing financial interests or personal relationships that could have appeared to influence the work reported in this paper.

REFERENCES

[1] A. D. Tura and H. B. Mamo, "Characterization and parametric optimization of additive manufacturing process for enhancing mechanical properties," *Heliyon*, vol. 8, no. 7, Jul. 2022, https://doi.org/10.1016/j.heliyon.2022.e09832.

[2] H. H. Abdulridha and T. F. Abbas, "Analyzing the Impact of FDM Parameters on Compression Strength and Dimensional Accuracy in 3D printed PLA Parts," *Engineering and Technology Journal*, vol. 41, no. 12, pp. 1611–1626, Dec. 2023, https://doi.org/10.30684/etj.2023.143615.1599.

[3] B. A. Hind, B. A. Haider, H. S. Mukhallad, and K. H. Saad, "Experimental investigation and statistical modelling for assessing the sliding wear of Futilized Filament Fabrication (FFF) fabricated parts," *Periodicals of Engineering and Natural Sciences*, vol. 11, no. 2, pp. 248–261, Apr. 2023, https://doi.org/10.21533/pen.v11.i2.116.

[4] A. A. Muhsan, H. B. Ali, M. S. Hamza, and R. A. Anaee, "Effect of nickel – Graphene addition on the 3D printed 17-4 PH stainless steel," *Results in Engineering*, vol. 20, Dec. 2023, Art. no. 101612, https://doi.org/10.1016/j.rineng.2023.101612.

[5] H. B. Ali, J. K. Oleiwi, and F. M. Othman, "Compressive and Tensile Properties of ABS Material as a Function of 3D Printing Process Parameters," *Journal of Composite and Advanced Materials*, vol. 32, no. 3, pp. 117–123, 2022, https://doi.org/10.18280/rcma.320302.

[6] D. Yadav, D. Chhabra, R. Kumar Garg, A. Ahlawat, and A. Phogat, "Optimization of FDM 3D printing process parameters for multi-material using artificial neural network," *Materials Today: Proceedings*, vol. 21, pp. 1583–1591, Jan. 2020, https://doi.org/10.1016/j.matpr.2019.11.225.

[7] S. Oudah, H. Al-Attraqchi, and N. Nassir, "The Effect of Process Parameters on the Compression Property of Acrylonitrile Butadiene Styrene Produced by 3D Printer," *Engineering and Technology Journal*, vol. 40, no. 1, pp. 189–194, Jan. 2022, https://doi.org/10.30684/etj.v40i1.2118.

[8] G. Wang, D. Zhang, B. Li, G. Wan, G. Zhao, and A. Zhang, "Strong and thermal-resistance glass fiber-reinforced polylactic acid (PLA) composites enabled by heat treatment," *International Journal of Biological Macromolecules*, vol. 129, pp. 448–459, May 2019, https://doi.org/10.1016/j.ijbiomac.2019.02.020.

[9] G. Wang, D. Zhang, G. Wan, B. Li, and G. Zhao, "Glass fiber reinforced PLA composite with enhanced mechanical properties, thermal behavior, and foaming ability," *Polymer*, vol. 181, Oct. 2019, Art no. 121803, https://doi.org/10.1016/j.polymer.2019.121803.

[10] K. Álvarez, R. F. Lagos, and M. Aizpun, "Investigating the influence of infill percentage on the mechanical properties of fused deposition modelled ABS parts," *Ingeniería e Investigación*, vol. 36, no. 3, pp. 110–116, Sep. 2016, https://doi.org/10.15446/ing.investig.v36n3.56610.

[11] M. Galeja, A. Hejna, P. Kosmela, and A. Kulawik, "Static and Dynamic Mechanical Properties of 3D Printed ABS as a Function of Raster Angle," *Materials*, vol. 13, no. 2, Jan. 2020, Art no. 297, https://doi.org/10.3390/ma13020297.

[12] M. Ramesh, L. Rajeshkumar, and D. Balaji, "Influence of Process Parameters on the Properties of Additively Manufactured Fiber-Reinforced Polymer Composite Materials: A Review," *Journal of Materials Engineering and Performance*, vol. 30, no. 7, pp. 4792–4807, Jul. 2021, https://doi.org/10.1007/s11665-021-05832-y.

[13] M. Somireddy and A. Czekanski, "Mechanical Characterization of Additively Manufactured Parts by FE Modeling of Mesostructure," *Journal of Manufacturing and Materials Processing*, vol. 1, no. 2, Dec. 2017, Art no. 18, https://doi.org/10.3390/jmmp1020018.

[14] M. F. Jasim, T. F. Abbas, and A. F. Huayier, "The Effect of Infill Pattern on Tensile Strength of PLA Material in Fused Deposition Modeling (FDM) Process," *Engineering and Technology Journal*, vol. 40, no. 12, pp. 1–8, Sep. 2022, https://doi.org/10.30684/etj.2021.131733.1054.

[15] N. Naveed, "Investigating the Material Properties and Microstructural Changes of Fused Filament Fabricated PLA and Tough-PLA Parts," *Polymers*, vol. 13, no. 9, Jan. 2021, Art no. 1487, https://doi.org/10.3390/polym13091487.

[16] M. Hikmat, S. Rostam, and Y. M. Ahmed, "Investigation of tensile property-based Taguchi method of PLA parts fabricated by FDM 3D printing technology," *Results in Engineering*, vol. 11, Sep. 2021, Art no. 100264, https://doi.org/10.1016/j.rineng.2021.100264.

[17] E. U. Enemuoh, S. Duginski, C. Feyen, and V. G. Menta, "Effect of Process Parameters on Energy Consumption, Physical, and Mechanical Properties of Fused Deposition Modeling," *Polymers*, vol. 13, no. 15, Jan. 2021, Art no. 2406, https://doi.org/10.3390/polym13152406.

[18] M. J. Martín, J. A. Auñón, and F. Martín, "Influence of Infill Pattern on Mechanical Behavior of Polymeric and Composites Specimens Manufactured Using Fused Filament Fabrication Technology," *Polymers*, vol. 13, no. 17, Jan. 2021, Art no. 2934, https://doi.org/10.3390/polym13172934.

[19] T. F. Abbas, A. Hind Basil, and K. K. Mansor, "Influence of Fdm Process Variables' on Tensile Strength, Weight, and Actual Printing Time When Using Abs Filament," *International Journal of Modern Manufacturing Technologies*, vol. 14, no. 1, pp. 7–13, Jun. 2022, https://doi.org/10.54684/ijmmt.2022.14.1.7.

[20] F. Baumann, J. Scholz, and J. Fleischer, "Investigation of a New Approach for Additively Manufactured Continuous Fiber-reinforced Polymers," *Procedia CIRP*, vol. 66, pp. 323–328, Jan. 2017, https://doi.org/10.1016/j.procir.2017.03.276.

[21] A. García-Domínguez, J. Claver, and M. A. Sebastián, "Infill optimization for pieces obtained by 3D printing," *Procedia Manufacturing*, vol. 41, pp. 193–199, Jan. 2019, https://doi.org/10.1016/j.promfg.2019.07.046.

[22] B. Aloyaydi, S. Sivasankaran, and A. Mustafa, "Investigation of infill-patterns on mechanical response of 3D printed poly-lactic-acid," *Polymer Testing*, vol. 87, Jul. 2020, Art no. 106557, https://doi.org/10.1016/j.polymertesting.2020.106557.

[23] N. Vidakis, A. Vairis, M. Petousis, K. Savvakis, and J. Kechagias, "Fused Deposition Modelling Parts Tensile Strength Characterisation," *Academic Journal of Manufacturing Engineering*, vol. 14, no. 2, pp. 87–94, 2016.

[24] A. Al Rashid and M. Koç, "Creep and Recovery Behavior of Continuous Fiber-Reinforced 3DP Composites," *Polymers*, vol. 13, no. 10, Jan. 2021, Art no. 1644, https://doi.org/10.3390/polym13101644.

[25] J. C. Camargo, Á. R. Machado, E. C. Almeida, and E. F. M. S. Silva, "Mechanical properties of PLA-graphene filament for FDM 3D printing," *The International Journal of Advanced Manufacturing Technology*, vol. 103, no. 5, pp. 2423–2443, Aug. 2019, https://doi.org/10.1007/s00170-019-03532-5.

[26] M. Harris, J. Potgieter, S. Ray, R. Archer, and K. M. Arif, "Acrylonitrile Butadiene Styrene and Polypropylene Blend with Enhanced Thermal and Mechanical Properties for Fused Filament Fabrication," *Materials*, vol. 12, no. 24, Jan. 2019, Art no. 4167, https://doi.org/10.3390/ma12244167.

[27] D. Popescu, A. Zapciu, C. Amza, F. Baciu, and R. Marinescu, "FDM process parameters influence over the mechanical properties of polymer specimens: A review," *Polymer Testing*, vol. 69, pp. 157–166, Aug. 2018, https://doi.org/10.1016/j.polymertesting.2018.05.020.

[28] R. E. Przekop, E. Gabriel, D. Pakuła, and B. Sztorch, "Liquid for Fused Deposition Modeling Technique (L-FDM)—A Revolution in Application Chemicals to 3D Printing Technology: Color and Elements," *Applied Sciences*, vol. 13, no. 13, Jan. 2023, Art no. 7393, https://doi.org/10.3390/app13137393.

[29] Z. H. Neamah, L. A. Al-Kindi, and G. Al-Kindi, "Design and manufacturing of custom 3D printed bone implants," *Engineering and Technology Journal*, vol. 42, no. 6, pp. 665–676, Jun. 2024, https://doi.org/10.30684/etj.2023.143788.1609.

[30] V. Shanmugam *et al.*, "The mechanical testing and performance analysis of polymer-fibre composites prepared through the additive manufacturing," *Polymer Testing*, vol. 93, Jan. 2021, Art no. 106925, https://doi.org/10.1016/j.polymertesting.2020.106925.

[31] Subcommittee: D20.10, "D638-22 Standard Test Method for Tensile Properties of Plastics." Jul. 21, 2022.

[32] P. A. Nayakappa, W. Gaurish, and G. Mahesh, "Grey Relation Analysis Methodology and its Application," *RESEARCH REVIEW International Journal of Multidisciplinary*, vol. 04, no. 02, pp. 409–411, 2015.

[33] A. R. Kafshgar, S. Rostami, M. Aliha, and F. Berto, "Optimization of Properties for 3D Printed PLA Material Using Taguchi, ANOVA and Multi-Objective Methodologies," *Procedia Structural Integrity*, vol. 34, pp. 71–77, Jan. 2021, https://doi.org/10.1016/j.prostr.2021.12.011.

[34] M. A. Abdullah and T. F. Abbas, "Investigation and Prediction of the Impact of FDM Process Parameters on Mechanical Properties of PLA Prints," *Engineering and Technology Journal*, vol. 41, no. 12, pp. 1465–1473, Aug. 2023, https://doi.org/10.30684/etj.2023.140389.1466.

[35] H. Hasani, S. A. Tabatabaei, and G. Amiri, "Grey Relational Analysis to Determine the Optimum Process Parameters for Open-End Spinning Yarns," *Journal of Engineered Fibers and Fabrics*, vol. 7, no. 2, Jun. 2012, Art no. 155892501200700212, https://doi.org/10.1177/155892501200700212.

[36] L. Yang, O. Harrysson, H. West, and D. Cormier, "Mechanical properties of 3D re-entrant honeycomb auxetic structures realized via additive manufacturing," *International Journal of Solids and Structures*, vol. 69–70, pp. 475–490, Sep. 2015, https://doi.org/10.1016/j.ijsolstr.2015.05.005.